

Optimization of LC Droplet Size and Electro-Optical Properties of Acrylate-Based Polymer-Dispersed Liquid Crystal by Controlling Photocure Rate

Jung-Dae Cho,¹ Sang-Sub Lee,¹ Su-Cheol Park,¹ Yang-Bae Kim,¹ Jin-Who Hong²

¹Institute of Photonics & Surface Treatment, Q-Sys Co. Ltd., Buk-Gu, Gwangju, Korea

²Department of Polymer Science & Engineering, Chosun University, Gwangju, Korea

Correspondence to: J.-W. Hong (E-mail: jhhong@chosun.ac.kr)

ABSTRACT: We investigated the effects of the different content ratios of 2-ethylhexylacrylate (2-EHA) and 2-ethylhexylmethacrylate (2-EHMA) on the relationships among the photopolymerization rate, morphology of liquid crystals (LCs) droplets, and electro-optical properties of trifunctional urethane acrylate-based polymer-dispersed liquid crystal (PDLC) systems. Photo-differential scanning calorimetry (DSC) analysis and resistivity measurement revealed that increasing 2-EHMA content gradually decreased the photocure rate of trifunctional urethane acrylate-based PDLCs, which prolonged the phase separation between the LC molecules and the prepolymers. Morphological observations and electro-optical measurements demonstrated that trifunctional urethane acrylate-based PDLCs with the 2-EHA:2-EHMA ratios from 4:1 to 3:2 in weight percent formed the favorable microstructures of LC droplets being within the range of 1–5 μm to scatter light efficiently and showed the satisfactory off-state opacity and on-state transmittance and the relatively low-driving voltage. The microstructures of LC droplets and electro-optical properties of trifunctional urethane acrylate-based PDLCs could be usefully optimized by controlling the photocure rate using the different 2-EHA/2-EHMA content ratios. © 2013 Wiley Periodicals, Inc. *J. Appl. Polym. Sci.* 130: 3098–3104, 2013

KEYWORDS: liquid crystals; morphology; photopolymerization; PDLC

Received 5 February 2013; accepted 14 May 2013; Published online 8 June 2013

DOI: 10.1002/app.39558

INTRODUCTION

Polymer-dispersed liquid crystals (PDLCs) are composites of randomly distributed microdroplets of liquid crystalline materials in a polymer matrix, formed by the phase separation of liquid crystal (LC) and polymer from a homogeneous single-phase mixture.^{1,2} The LC domains can provide electro-optically controllable functions because of their orientation being influenced by an applied electrical field, whereas the polymer matrix provides mechanical, thermal, and environmental stability. In the off-state, a PDLC composite appears opaque because it strongly scatters light because of the refractive index mismatch between the LC droplets and the polymer matrix, whereas in the on-state a PDLC becomes transparent because it allows light to pass because of the reorientation of LC within the droplets and matching of the refractive indices of LC and polymer.^{3–9} The intrinsic ability of PDLC to modulate light (scattering mode) means that it has potential applications in various electro-optical devices, such as switchable privacy windows (smart windows), optical shutters, tunable LC lenses, flexible displays, projection displays, and other light-control devices.^{10–20}

PDLC can be manufactured using various methods, including microencapsulation, polymerization-induced phase separation (PIPS), thermally induced phase separation, and solvent-induced phase separation. Photoinitiated PIPS systems have proven to be a most versatile and useful phase-separation method of fabricating PDLC composites because of it being relatively simple, clean, and solvent-free. Acrylate systems undergoing chain-growth radical polymerization and thiol–ene systems undergoing step-growth polymerization have been the most widely applied materials in photopolymerization processes employing the photoinitiated PIPS method for PDLC formation.^{2,21–25}

The use of acrylates and methacrylates in PDLC systems was first reported by Hirai et al.,^{2,26} and since then many research groups have reported photopolymerizable PDLC composites using acrylate photochemistry to generate the polymer matrix in various electro-optical applications.^{27–37} The associated studies have mainly investigated the phase separation kinetics, electro-optical properties, and morphological development in acrylate-based PDLC systems useful for different electro-optical applications by adjusting various parameters, such as the

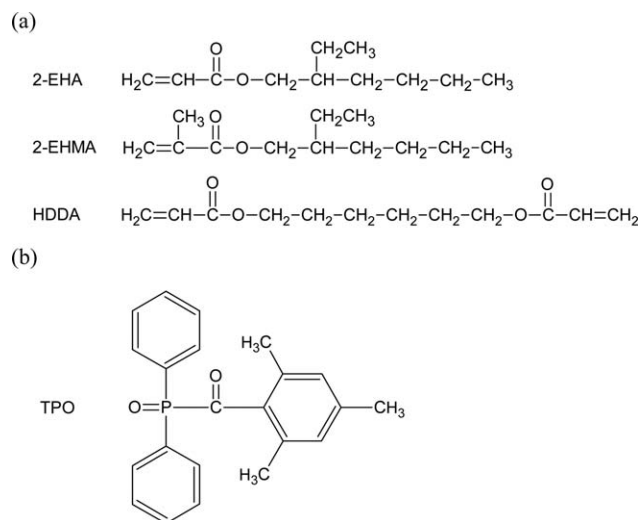


Figure 1. Chemical structures of (a) the monomers and cross-linker and (b) the photoinitiator.

different types and concentrations of LC and prepolymer, the addition of various reinforcing materials, UV intensity, curing temperature, film thickness, and so on.^{38–42}

Compared to thiol–ene systems, acrylates provide good solubility with the LC, good storage stability, and wide selection of materials to form the polymer matrix in PDLC systems.² Especially, the use of multifunctional acrylate monomers or oligomers in PDLC mixtures gives good mechanical properties and thermal stability to the UV-cured PDLC composites. However, the one major drawback of multifunctional acrylates is the fast rates of cure and phase separation, which causes the polymer ball morphology or the submicron-sized LC droplets within the polymer matrix. PDLC composites with such morphologies tend to exhibit large memory effects, high-driving voltage, and inefficient light scattering.^{2,25}

Therefore, we have considered a simple and useful method of controlling the microstructures of LC droplets in multifunctional acrylate-based PDLC systems by adjusting the photocure rate using the content ratios of monofunctional acrylate and methacrylate monomers to optimize the favorable sizes of the LC droplets and electro-optical properties. The accurate control of the microstructures of LC droplets is a very important factor because it determines the morphological and electro-optical properties of acrylate-based PDLC systems.

In this study, we investigated the effects of the different content ratios of 2-ethylhexylacrylate (2-EHA) and 2-ethylhexylmethacrylate (2-EHMA) on the relationships among the photocure rate, morphology, and electro-optical properties of trifunctional urethane acrylate-based PDLC systems by using photo-differential scanning calorimetry (photo-DSC), resistivity measurement, scanning electron microscopy (SEM), and electro-optical measurement.

EXPERIMENTAL

Materials

Aliphatic urethane triacrylate oligomer (EB 264, SK-CYTEC), 2-EHA (Aldrich), and 2-EHMA (Aldrich) were used as a resin

and monomers, respectively. 1,6-Hexanediol diacrylate (Aldrich) was used as a cross-linker and 2,4,6-trimethylbenzoyl-diphenylphosphineoxide (Ciba Specialty Chemicals) was used as a photoinitiator. A multicomponent eutectic LC mixture of cyanobiphenyls (E7, Merck) was used as a nematic LC. This mixture comprises of 51% *n*-pentylcyanobiphenyl, 25% *n*-heptylcyanobiphenyl, 16% *n*-octyloxycyanobiphenyl, and 8% *n*-pentylcyanoterphenyl and has a nematic mesophase from -30°C to 61°C .^{16,20} All the chemicals were used as received without further purification; the chemical structures of the monomers, cross-linker, and photoinitiator are presented in Figure 1.

Preparation of Prepolymer Formulations and PDLC Sample Cells

Various prepolymer formulations (designated A–F) were prepared by varying the concentrations of 2-EHA and 2-EHMA (as listed in Table I). The mixtures for the PDLC sample cells were prepared by directly mixing 60 wt % E7 with each prepolymer formulation (A–F) at 40 wt % over 5 h at room temperature; these were used as the initial reactive mixtures for UV curing. The PDLC sample cells were prepared by sandwiching the initial reactive mixtures between two conductive ITO-coated glass plates ($60 \times 50 \text{ mm}^2$). The cell gap was adjusted to $10 \mu\text{m}$ by using polymer ball spacers. The PDLC samples were irradiated by a black-light lamp (ENF-240, Spectronics) at a light intensity of 1.0 mW/cm^2 at 365 nm for 3 min.

Photo-DSC

The photo-DSC experiments were performed using a DSC equipped with a photocalorimetric accessory (TA 5000/DPC System). The initiation light source was a black-light lamp (ENF-240, Spectronics) that irradiated the sample at a light intensity of 1.0 mW/cm^2 at 365 nm . Samples weighing $1.0 \pm 0.1 \text{ mg}$ (mean \pm SD) were placed in uncovered aluminum pans, and a reference aluminum pan was left empty. All photocuring experiments were performed at an isothermal temperature of 25°C . The exothermic value achieved for the photocuring at 100°C was 355 J/g and this was considered to be the total heat (ΔH_{total}) for the fully cured PDLC composite. This value was used in the subsequent analysis, and all photo-DSC thermograms of PDLC samples were normalized by the mass of the

Table I. Prepolymer Formulations with Varying Monomer Contents

Component	A	B	C	D	E	F
EB 264 ^a	70	70	70	70	70	70
2-EHA ^b	25	20	15	10	5	0
2-EHMA ^b	0	5	10	15	20	25
HDDA ^b	5	5	5	5	5	5
TPO ^c	1	1	1	1	1	1

Data values represent weight percentages.

2-EHA, 2-ethylhexylacrylate; 2-EHMA, 2-ethylhexylmethacrylate; HDDA, 1,6-hexanediol diacrylate; TPO, 2,4,6-trimethylbenzoyl diphenylphosphine oxide.

^a SK-CYTEC.

^b Aldrich.

^c Ciba Specialty Chemicals.

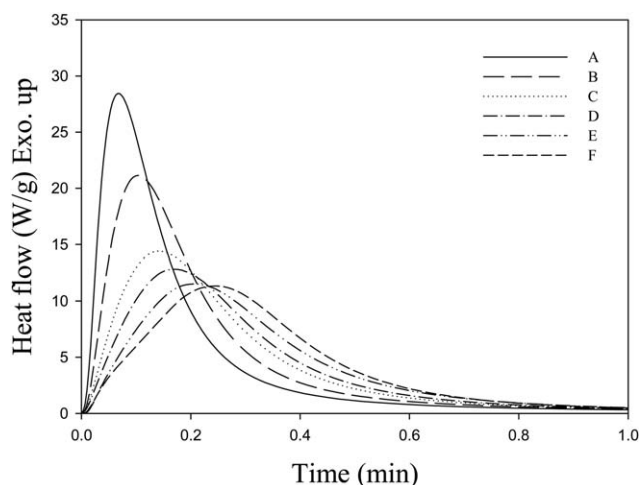


Figure 2. Photo-DSC exotherms for the photopolymerization of PDLC compounds A–F.

prepolymer. TA Instruments software was used to obtain the data values in the photo-DSC experiments.

Resistivity Measurement

An experimental setup equipped with a resistivity meter (Megaresta H0709, Shishido Electrostatic Ltd.) and a black-light lamp (ENF-240, Spectronics) with a light intensity of 1.0 mW/cm² at 365 nm was used to measure the resistance of the PDLC sample cells during the photopolymerization process under room temperature.

Scanning Electron Microscopy

The surface morphology of the polymer matrix in the PDLC samples was observed using scanning electron microscopy (SEM; Hitachi S-4700) at an accelerating voltage of 5 kV. The glass substrates were carefully removed and the remaining composite layer was dipped in hexane for 24 h at room temperature to extract the LC molecules, and then the polymer matrix was dried in a vacuum for 24 h to remove the solvent. The microstructure of the polymer matrix was observed under SEM after the polymer matrix had been sputtered with gold.

Electro-Optical Measurement

An experimental setup equipped with a halogen lamp (AvaLight-Hal, Avantes) as an incident light source, CCD detector (AvaSpec-2048, Avantes), and rotating sample stage was used to monitor the parallel light transmittance of the PDLC sample cells at 650 nm. The collection angle of the transmitted light was about $\pm 3^\circ$. Curves of the applied voltage (V) versus transmittance (T) were obtained by applying an external electric field across the PDLC samples. In this process, a 60-Hz sinusoidal voltage was stepwise increased up to the saturation level and then decreased stepwise back to the baseline value. The driving voltage (V_d) was defined as that used to produce the electric field required for the transmittance to reach the onset of saturation (T_s).

RESULTS AND DISCUSSION

Photocure Kinetics

The cure kinetics was evaluated using photo-DSC to clarify the photopolymerization process of the various trifunctional

urethane acrylate-based PDLC compounds. Photo-DSC experiments can provide kinetics data in which the measured heat flow can be converted directly into the ultimate percentage conversion and polymerization rate for a given formulation, with the data obtained reflecting the overall curing reaction of the sample.^{43–47}

The photo-DSC method assumes that the heat flow measured in a curing process is proportional to the conversion rate. This assumption is valid for materials exhibiting a single reaction or no other enthalpic events, such as the evaporation of solvent or volatile components, enthalpy relaxation, or significant changes in heat capacity with conversion. The rate of change in the conversion can therefore be defined as follows^{48–50}:

$$\frac{d\alpha}{dt} = \frac{1}{\Delta H_{\text{total}}} \left(\frac{dH}{dt} \right)_T, \quad (1)$$

where $d\alpha/dt$ is the conversion or polymerization rate, ΔH_{total} is the total exothermic heat of reaction, and $(dH/dt)_T$ is the measured heat flow at a constant temperature T . The degree of conversion is obtained by integrating eq. (1):

$$\alpha = \frac{1}{\Delta H_{\text{total}}} \int_0^t \left(\frac{dH}{dt} \right)_T dt, \quad (2)$$

where α is the degree of conversion. In this definition the resin is considered to be uncured when $\alpha = 0$ and completely cured when $\alpha = 1$.

For simplifying the analysis of trifunctional urethane acrylate-based PDLC systems with different 2-EHA/2-EHMA ratios (see Table I), it was necessary to fix the contents of the two oligomer and cross-linker components, and only change the monomer contents. Each PDLC compound contained 60 wt % E7 and 40 wt % prepolymer with various contents of 2-EHA and 2-EHMA, and the 2-EHA:2-EHMA ratio was varied from 25:0 to 0:25.

Figure 2 presents the photo-DSC exotherms for the photopolymerization of urethane acrylate-based PDLC compounds A–F. Plots of the percentage conversion versus irradiation time

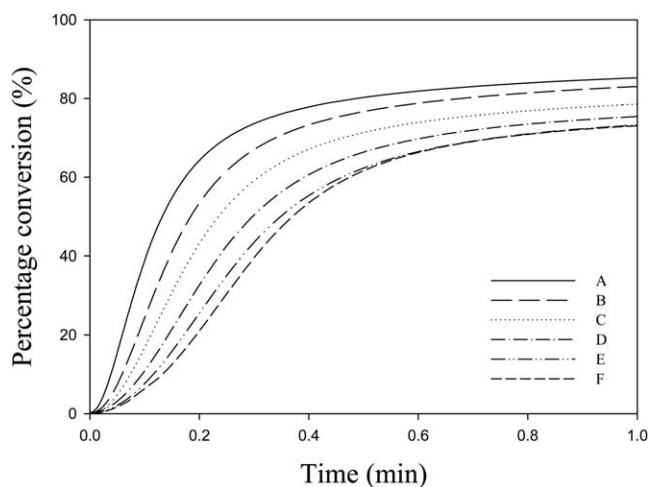


Figure 3. Percentage conversion profiles for the photopolymerization of PDLC compounds A–F.

Table II. Kinetics Analysis Results for the Photopolymerization of PDLC Compounds A–F

Compound	ΔH (J/g)	Conversion (%)	Induction time (s)	Peak maximum (min)	$R_{p,max}$ (min^{-1})
A (0 wt % ^a)	298	84	1.74	0.07	4.94
B (5 wt %)	291	82	2.17	0.10	3.65
C (10 wt %)	273	77	2.42	0.14	2.81
D (15 wt %)	261	74	2.61	0.17	2.28
E (20 wt %)	255	72	2.87	0.21	1.98
F (25 wt %)	256	72	3.00	0.25	1.89

$R_{p,max}$, maximum polymerization rate ($R_p = dx/dt$, where x is the fraction of resin converted).
^a2-EHMA content.

derived from Figure 2 for the photopolymerization of PDLC compounds A–F are shown in Figure 3. This figure indicates that the conversion versus time kinetics curves of all of the PDLC compounds studied were indicative of autoaccelerated processes, which are a typical feature of an autocatalytic reaction mechanism. The amounts of heat released, ultimate percentage conversions, induction times, peak maxima, and maximum polymerization rates ($R_{p,max}$) derived from Figures 2 and 3 are collected in Table II. Here, it should be noted that the exotherm and the degree of conversion are related to the cure extent, and the induction time, peak maximum, and $R_{p,max}$ are related to the cure rate.

From the viewpoint of the overall cure extent, increasing the concentration of 2-EHMA caused the exotherm and percentage conversion to decrease steadily and then level off, which indicates that higher 2-EHMA content decreased the cross-link density of the polymer network within the UV-cured trifunctional urethane acrylate-based PDLC composite. In terms of the overall cure rate, increasing the concentration of 2-EHMA increased the induction time (which is the time to attain a conversion of 1%, and is related to the efficiency of the photoinitiator) and the peak maximum (which is the time to attain the exotherm maximum), but decreased $R_{p,max}$, shows that higher 2-EHMA content decreased the photopolymerization rate of the PDLC compound. As expected, adding 2-EHMA decreased both the overall cure extent and the cure rate of trifunctional urethane acrylate-based PDLC systems, probably because of methacrylates being less reactive than acrylates.⁵¹ The presence of 2-EHMA clearly affected the photocure behaviors of the trifunctional urethane acrylate-based PDLC compounds. Therefore, the derived phenomena are both important and notable because the related kinetics results indicate the possibility of controlling the photocure rate, LC droplet size, and electro-optical properties of trifunctional urethane acrylate-based PDLC systems by varying the content ratios of 2-EHA and 2-EHMA.

Another experiment was performed to clarify the effect of the contents of 2-EHA and 2-EHMA on the photocure behaviors of trifunctional urethane acrylate-based PDLC systems using resistivity measurement. Figure 4 exhibits the UV-curing time dependencies of the resistivity of the PDLC sample cells A–F. Figure 4 indicates that according to the UV-curing time the resistivity of PDLC cell A without 2-EHMA sharply increased, whereas for the PDLC cell F with 25 wt % 2-EHMA showed the

slowest increase, which means that the cross-linking density of the polymer network within the UV-cured PDLC composite gradually decreased with increasing 2-EHMA content in the present PDLC formulation systems. This resistivity measurement result is in accordance with the data of the amounts of heat released and the ultimate percentage conversions obtained by the photo-DSC experiments.

Morphological and Electro-Optical Properties

The photopolymerization conditions under which photoinitiated PDLC composites are fabricated have a dramatic impact on their physicochemical and mechanical properties. In particular, the photocure rate determines the morphological and electro-optical properties such as the microstructures of LC droplets, the light transmittance, the driving voltage, and the phase separation behavior between the prepolymer and the LC molecules. Therefore, the control of the photocure rate plays a key role in the formation of the favorable LC droplet size, strong light scattering, and low-driving voltage for the PDLC systems. In the previous section, we examined the effect of the content ratios of 2-EHA and 2-EHMA on the photocure kinetics of trifunctional urethane acrylate-based PDLC system using photo-DSC. Then, in this section, we will address how the content ratios of 2-EHA and 2-EHMA influenced the relationships among the photocure rate, the morphology, and the

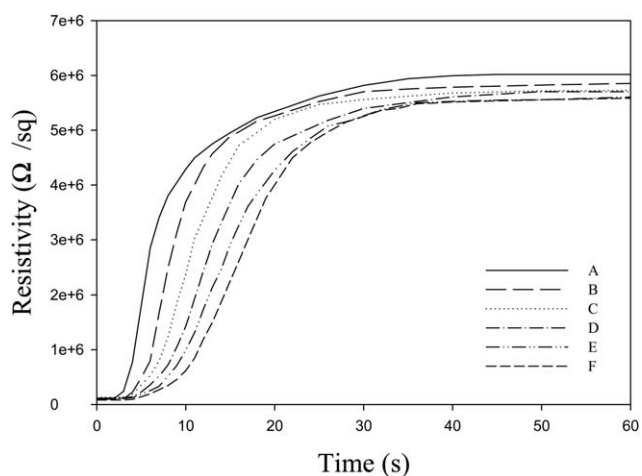


Figure 4. Curves of resistivity versus UV-curing time for PDLC sample cells A–F.

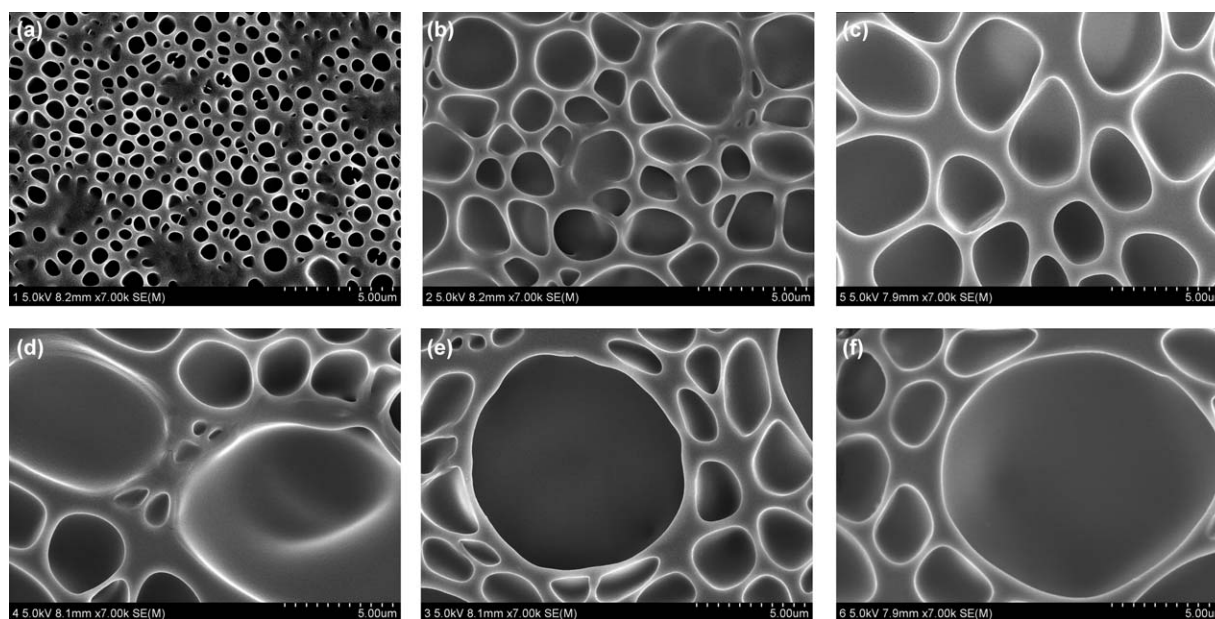


Figure 5. SEM photographs of the surface of the polymer matrix of the PDLC samples with various 2-EHMA concentrations (the scale bar is 5 μm in length.): (a) A (0 wt %), (b) B (5 wt %), (c) C (10 wt %), (d) D (15 wt %), (e) E (20 wt %), and (f) F (25 wt %).

electro-optical properties of the PDLC composites using SEM and electro-optic measurements.

Figure 5 shows SEM photographs of the surface of the polymer matrix of the trifunctional urethane acrylate-based PDLC samples with various content ratios of 2-EHA and 2-EHMA. Figure 5 clearly shows that increasing the 2-EHMA content increased the size of LC droplets within the UV-cured polymer matrix, which means that slowing the photocure rate of the prepolymer prolonged the phase separation time between the LC molecules and the prepolymer. Notably, there was a marked increase in the number of LC droplets larger than 5 μm in PDLC composites containing more than 15 wt % 2-EHMA. Generally, LC droplets tend to have diameters ranging from 0.1 to 10 μm irrespective of the PDLC manufacturing process, with 1–3 μm droplets being the most common. In addition, PDLC composites containing submicron-sized LC droplets do not scatter light very efficiently; neither do composites containing very large droplets above 10 μm . For optimum light scattering with a milky-white appearance and satisfactory off-state opacity properties, the LC droplet diameter should be within the range of 1–2 μm or at least 1–5 μm .^{2,25} As shown in the morphological measurement in Figure 5, the PDLC composites containing 5–10 wt % 2-EHMA exhibited the favorable microstructures of LC droplets being within the range of 1–5 μm .

To investigate the relationship between the morphological and electro-optical properties of trifunctional urethane acrylate-based PDLC composites, the voltage dependencies of the transmittance of PDLC sample cells A–F are shown in Figure 6, with the obtained data values listed in Table III. Here, T_0 is the initial off-state transmittance and increasing the applied voltage increased the transmittance of the PDLC samples until it eventually reached T_s . The driving voltage (V_d) was defined

according to the electric field required for the transmittance to reach T_s in this study. Figure 6 and Table III represent that T_0 decreased slightly for the 2-EHMA contents up to 10 wt %, and then increased dramatically for the 2-EHMA contents above 15 wt %. As shown in Figures 5 and 6, it was clear from the morphological observations and electro-optical properties that PDLC sample cells B and C formed the LC droplet diameter being within the range of 1–5 μm to scatter light efficiently, exhibiting low T_0 , that is, satisfactory off-state opacity. However, T_0 increased sharply when the 2-EHMA content exceeded 15 wt %, probably because of the presence of many LC droplets larger than 5 μm , which resulted in poor light scattering. In addition, T_0 was slightly higher for PDLC sample cell A without 2-EHMA than for sample cells B and C, and gave rise to a reddish hue

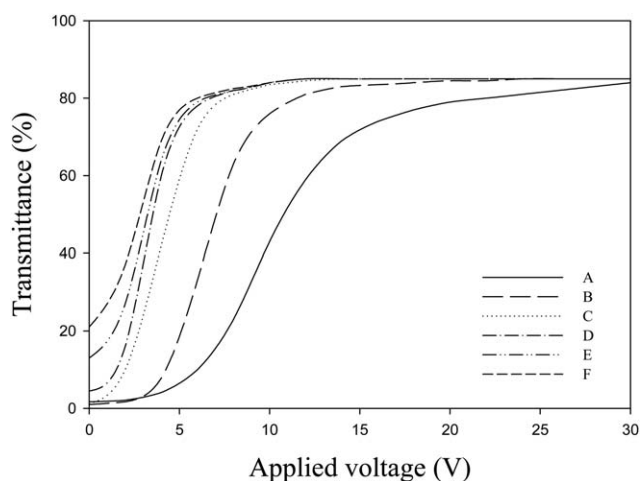


Figure 6. Curves of transmittance at 650 nm vs. voltage for PDLC sample cells A–F.

Table III. Electro-Optical Properties of PDLC Sample Cells A–F

Sample cell	Transmittance (%)		V_d (V)
	T_o	T_s	
A (0 wt % ^a)	1.7	84	30
B (5 wt %)	1.0	85	24
C (10 wt %)	1.2	85	14
D (15 wt %)	4.5	85	12
E (20 wt %)	13.0	85	12
F (25 wt %)	21.0	85	12

T_o , initial off-state transmittance; T_s , transmittance at the saturation level; V_d , driving voltage defined as the electric field required to reach T_s .
^a 2-EHMA content.

owing to the “red bleed-through” effect caused by the submicron-sized LC droplets mostly smaller than 1 μm .² This “red bleed-through” phenomenon can be explained by the fact that such size scales will preferentially scatter blue light, thus leaving red light to pass through, which would cause a red hue in the transmission. Expectedly, the trifunctional urethane acrylate-based PDLC system without 2-EHMA showed the fastest photocure rate during the photopolymerization process, as given in Table II, which led to the insufficient phase separation between the LC molecules and the prepolymer and the formation of many submicron-sized LC droplets within the polymer matrix, and eventually exhibited the insufficient light scattering and the highest driving voltage. However, the PDLC systems of 5–10 wt % 2-EHMA showed moderate photocure rates to give the sufficient phase separation, which yielded good light scattering and off-state opacity properties.

Meanwhile, V_d decreased dramatically as the 2-EHMA content increased up to 15 wt %, and then leveled off. This trend indicates that the driving voltage required to switch a PDLC cell varies with the LC droplet size, the submicron-sized LC droplets required higher electric-field strengths to align the LC molecules, and the LC droplets larger than 5 μm did not contribute to a further decrease in the driving voltage and made the off-state opacity properties even worse in these PDLC systems. Therefore, considering the morphological and electro-optical properties of trifunctional urethane acrylate-based PDLC system with the different content ratios of 2-EHA and 2-EHMA, PDLC composites with the 2-EHA:2-EHMA ratios from 4:1 to 3:2 in weight percent showed the favorable microstructures of LC droplets, the satisfactory off-state opacity and on-state transmittance, and the relatively low-driving voltage.

In this study, the appropriate content ratios of monofunctional 2-EHA and 2-EHMA monomers to the multifunctional urethane acrylate-based PDLC system not only would help to control the rates of photocure and phase separation for the optimization of LC droplet sizes and electro-optical properties, but also could be used to overcome the major drawback of multifunctional acrylates forming the polymer ball morphology or the submicron-sized LC droplets within the polymer matrix because of their fast cure rate.

CONCLUSIONS

The effects of the different content ratios of 2-EHA and 2-EHMA on the photocure rate, morphology, and electro-optical properties of trifunctional urethane acrylate-based PDLC systems have been elucidated using photo-DSC, resistivity measurement, SEM, and electro-optical measurements. Photo-DSC analysis revealed that increasing the 2-EHMA content gradually slowed the cure reaction and cure rate of trifunctional urethane acrylate-based PDLC systems, which was supported by the resistivity measurement. The morphological observations revealed that increasing the 2-EHMA content increased the size of the LC droplets within the UV-cured polymer matrix, which means that the slower cure rate of prepolymer prolonged the phase separation time between the LC molecules and the prepolymer, thereby leading to the formation of large LC droplets. It was clear from the morphological and electro-optical properties that the trifunctional urethane acrylate-based PDLC systems with the 2-EHA:2-EHMA ratios from 4:1 to 3:2 in weight percent formed the favorable microstructures of LC droplets being within the range of 1–5 μm to scatter light efficiently and showed the satisfactory off-state opacity and on-state transmittance and the relatively low-driving voltage. Lastly, it was found that the content ratios of 2-EHA and 2-EHMA played a simple and useful key role in controlling the photocure rate, phase separation rate, microstructures of LC droplets, and electro-optical properties of trifunctional urethane acrylate-based PDLC systems.

ACKNOWLEDGMENT

This study was supported by research fund from Chosun University in 2009.

REFERENCES

1. Doane, J. W. In *Liquid Crystals: Applications and Uses*; Bahadur, B., Ed.; World Scientific: Singapore, **1990**; p 361.
2. Drzaic, P. S. *Liquid Crystal Dispersions*; World Scientific: Singapore, **1995**.
3. Kajiyama, T.; Washizu, S.; Takayanagi, M. *J. Appl. Polym. Sci.* **1984**, *29*, 3955.
4. Kajiyama, T.; Washizu, S.; Ohomori, Y. *J. Membr. Sci.* **1985**, *24*, 73.
5. Doane, J. W.; Vaz, N. A.; Wu, B. G.; Zumer, S. *Appl. Phys. Lett.* **1986**, *48*, 269.
6. Drzaic, P. S. *J. Appl. Phys.* **1986**, *60*, 2142.
7. Montgomery Jr., G. P.; Vaz, N. A. *Phys. Rev. A* **1989**, *40*, 6580.
8. Montgomery Jr., G. P.; West, J. L.; Tamura-Lis, W. *J. Appl. Phys.* **1990**, *69*, 1605.
9. Whitehead Jr., J. B.; Zumer, S.; Doane, J. W. *J. Appl. Phys.* **1992**, *73*, 1057.
10. Coates, D. *Displays* **1993**, *14*, 94.
11. Kim, B. K.; Kim, S. H.; Song, J. C. *Polymer* **1998**, *39*, 5949.
12. Fujisawa, T.; Hayasi, M.; Nakada, H.; Tani, Y.; Aizawa, M. *Mol. Cryst. Liq. Cryst.* **2001**, *366*, 107.
13. Hoyle, C. E.; Lee, T. Y.; Roper, T. *J. Polym. Sci. Part A Polym. Chem.* **2004**, *42*, 5301.

14. Doane, J. W. *Liq. Cryst.* **2006**, *33*, 1313.
15. Wu, B. G.; Erdmann, J. H.; Doane, J. W. *Liq. Cryst.* **2006**, *33*, 1315.
16. Senyurt, A. F.; Warren, G.; Whitehead Jr., J. B.; Hoyle, C. E. *Polymer* **2006**, *47*, 2741.
17. Wang, P. C.; MacDiarmid, A. G. *Displays* **2007**, *28*, 101.
18. Shim, S. S.; Cho, Y. H.; Yoon, J. H.; Kim, B. K. *Eur. Polym. J.* **2009**, *45*, 2184.
19. Hadjichristov, G. B.; Marinov, Y. G.; Petrov, A. G. *Mol. Cryst. Liq. Cryst.* **2010**, *525*, 128.
20. Yaroshchuk, O.; Elouali, F.; Maschke, U. *Opt. Mater.* **2010**, *32*, 982.
21. Zhang, W.; Lin, J.; Yu, T.; Lin, S.; Yang, D. *Eur. Polym. J.* **2003**, *39*, 1635.
22. Yang, D.; Lin, J.; Li, T.; Lin, S.; Tian, X. *Eur. Polym. J.* **2004**, *40*, 1823.
23. Seok, J. W.; Ryu, H. S.; Seo, H. J.; Kim, W. S.; Lee, D. H.; Min, K. E.; Seo, K. H.; Kang, I. K.; Park, L. S. *Opt. Mater.* **2002**, *21*, 633.
24. Seok, J. W.; Han, Y. S.; Kwon, Y. H.; Park, L. S. *J. Appl. Polym. Sci.* **2006**, *99*, 162.
25. Li, W.; Cao, Y.; Cao, H.; Kashima, M.; Kong, L.; Yang, H., J. *Polym. Sci. Part B Polym. Phys.* **2008**, *46*, 1369.
26. Hirai, Y.; Niiyama, S.; Kumaim, H.; Gunjima, T. *Proc. SPIE*, **1990**, *1257*, p 2.
27. Coates, D.; Greenfield, S.; Goulding, M.; Brown, E.; Nolan, P. *Proc. SPIE*, **1993**, *1911*, p 2.
28. Bunning, T. J.; Natarajan, L. V.; Tondiglia, V. P.; Sutherland, R. L.; Vezie, D. L.; Adams, W. W. *Polymer* **1995**, *36*, 2699.
29. White, T. J.; Guymon, C. A. *Polym. Mater. Sci. Eng.* **2003**, *89*, 452.
30. Jung, J. A.; Kim, B. K.; Kim, J. C. *Eur. Polym. J.* **2006**, *42*, 2667.
31. Hwang, S. H.; Yang, K. J.; Woo, S. H.; Choi, B. D.; Kim, E. H.; Kim, B. K. *Mol. Cryst. Liq. Cryst.* **2007**, *470*, 163.
32. White, T. J.; Natarajan, L. V.; Bunning, T. J.; Guymon, C. A. *Liq. Cryst.* **2007**, *34*, 1377.
33. Jeon, Y. J.; Bingzhu, Y.; Rhee, J. T.; Cheung, D. L.; Jamil, M. *Macromol. Theory Simul.* **2007**, *16*, 643.
34. Hatice, D.; Scott, M.; Namil, K.; Jun, H.; Thein, K.; Lalgudi, V. N.; Vincent, P. T.; Timothy, J. B. *Polymer* **2008**, *49*, 534.
35. Koo, J. J.; No, Y. S.; Jeon, C. W.; Kim, J. H. *Mol. Cryst. Liq. Cryst.* **2008**, *491*, 58.
36. No, Y. S.; Jeon, C. W. *Mol. Cryst. Liq. Cryst.* **2009**, *513*, 98.
37. Abdoune, F. Z.; Benkhaled, L.; Mechernene, L.; Maschke, U. *Phys. Proc.* **2009**, *2*, 643.
38. Li, W.; Zhang, H.; Wang, L.; Ouyang, C.; Ding, X.; Cao, H.; Yang, H. *J. Appl. Polym. Sci.* **2007**, *105*, 2185.
39. Li, W.; Zhu, M.; Ding, X.; Li, B.; Huang, W.; Cao, H.; Yang, Z.; Yang, H. *J. Appl. Polym. Sci.* **2009**, *111*, 1449.
40. Kashima, M.; Cao, H.; Meng, Q.; Liu, H.; Wang, D.; Li, F.; Yang, H. *J. Appl. Polym. Sci.* **2010**, *117*, 3434.
41. Kim, E. H.; Myoung, S. W.; Lee, W. R.; Jung, Y. G. *J. Korean Phys. Soc.* **2009**, *54*, 1180.
42. Myoung, S. W.; Kim, E. H.; Jung, Y. G. *Thin Solid Films* **2010**, *519*, 1558.
43. Clark, S. C.; Hoyle, C. E.; Jönsson, S.; Morel, F.; Decker, C. *Polymer* **1999**, *40*, 5063.
44. Cho, J. D.; Hong, J. W. *J. Appl. Polym. Sci.* **2005**, *97*, 1345.
45. Cho, J. D.; Ju, H. T.; Hong, J. W. *J. Polym. Sci. Part A Polym. Chem.* **2005**, *43*, 658.
46. Cho, J. D.; Ju, H. T.; Park, Y. S.; Hong, J. W. *Macromol. Mater. Eng.* **2006**, *291*, 1155.
47. Cho, J. D.; Han, S. T.; Hong, J. W. *Polym. Test.* **2007**, *26*, 71.
48. Keenan, M. R. *J. Appl. Polym. Sci.* **1987**, *33*, 1725.
49. Nam, J. D.; Seferis, J. C. *J. Appl. Polym. Sci.* **1993**, *50*, 1555.
50. Boey, F. Y. C.; Qiang, W. *Polymer* **2000**, *41*, 2081.
51. Allen, N. S.; Johnson, M. S.; Oldring, P. K. T.; Salim, S. In *Chemistry & Technology of UV & EB Formulation for Coatings Inks & Paints*, Vol. 2; Oldring, P. K. T., Ed.; SITA Technology: London, **1991**; p 237.